

NN-AE-VQE: Neural network parameter prediction on autoencoded variational quantum eigensolvers

Koen J. Mesman,^{†,§} Yinglu Tang,^{†,§} Matthias Möller,^{†,‡} Boyang Chen,^{†,§} and
Sebastian Feld^{*,†,¶}

[†]*QAIMS, Delft University of Technology, Delft*

[‡]*Applied Mathematics, Delft University of Technology*

[¶]*Quantum Computing and Engineering, Delft University of Technology*

[§]*Aerospace Engineering, Delft University of Technology*

E-mail: @tudelft.nl

Abstract

A longstanding computational challenge is the accurate simulation of many-body particle systems. Especially for deriving key characteristics of high-impact but complex systems such as battery materials and high entropy alloys (HAE). While simple models allow for simulations of the required scale, these methods often fail to capture the complex dynamics that determine the characteristics. A long-theorized approach is to use quantum computers for this purpose, which allows for a more efficient encoding of quantum mechanical systems. In recent years, the field of quantum computing has become significantly more mature. Furthermore, the rise in integration of machine learning with quantum computing further pushes to a near-term advantage. In this work we aim to improve the well-established quantum computing method for calculating

the inter-atomic potential, the variational quantum eigensolver, by presenting an auto-encoded VQE with neural-network predictions: NN-AE-VQE. We apply a quantum autoencoder for a compressed quantum state representation of the atomic system, to which a naive circuit ansatz is applied. This reduces the number of circuit parameters to optimize, while still minimal reduction in accuracy. Additionally, we train a classical neural network to predict the circuit parameters to avoid computationally expensive parameter optimization. We demonstrate these methods on a H_2 molecule, achieving chemical accuracy. We believe this method shows promise of efficiently capturing highly accurate systems while omitting current bottlenecks of variational quantum algorithms. Finally, we explore options for exploiting the algorithm structure and further algorithm improvements.

1 Introduction

Novel materials are crucial for improving high-impact applications such as energy storage and aerospace heat protection systems. To find the required characteristics of a material configuration, a molecular dynamics (MD) simulation is performed. However, this can prove to be a challenge as the nature of these material characteristics can be complex, for example in high entropy ceramics.^{1,2} To determine the characteristics of such complex materials, the simulations need to capture the underlying dynamics accurately. It is therefore essential that the interaction between atoms (inter-atomic potential) is calculated precisely and efficiently.³

However, achieving the desired accuracy at the MD scale is a considerable challenge. MD simulations are generally performed for sample size and duration in the order of μm and μs .⁴ As such samples calculate the interaction of thousands of atoms, the computation time of these calculations becomes a serious bottleneck. While efficient methods exist, such as force fields ($O(N)$ for n electrons), these are too inaccurate for the targeted application. More accurate methods such as Density Functional Theory (DFT) and Unitary Coupled Cluster Single and Doubles (UCCSD)⁵ are computationally too costly ($O(n^3)$) and ($O(n^7)$)

respectively).⁶ This makes accurate simulations on a molecular dynamics scale intractable.

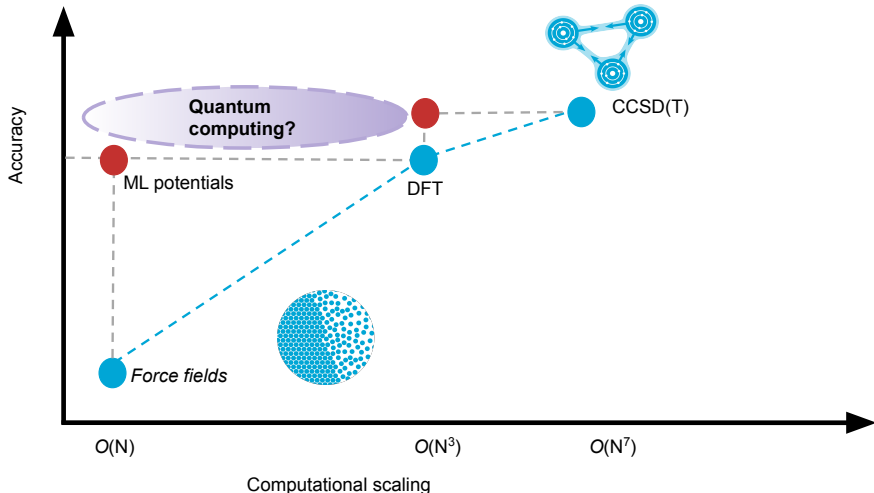


Figure 1: Computational complexity and accuracy trade-off comparison of direct computations (Force fields, DFT, CCSD(T)), machine learning potentials. The goal of using quantum computing is to improve this trade-off, but this has yet to be reached.

To improve the runtime/accuracy trade-off, data-based machine learning models of inter-atomic potentials have been developed.^{3,7,8} These models rely on high-fidelity calculations or experimental data to train e.g. a neural network to predict the inter-atomic potential. Machine learning potentials have been demonstrated to significantly reduce the computational cost compared to conventional calculations (see also Figure 1).³ However, challenges here are prevalent regarding model transferability, accuracy, or training data requirements.^{3,6,8} Especially when considering long-range effects, machine learning potentials have limited performance.⁶ Increasing the range of interactions, therefore increasing the number of atoms in the calculation, again makes the simulation intractable.

As such, we need a different computing paradigm to speed up calculations without losing accuracy. A long-theorized approach to simulating atomic systems with these benefits is quantum computing. This potentially achieves a more efficient encoding of the quantum mechanical preparation of the molecular system.^{9,10} Furthermore, quantum computing fun-

damentally computes entanglement (many-body interaction) more efficiently than classical methods. In doing so, the modeling of the system would be highly accurate, without the lengthy computational cost.

Currently, quantum computers do not have the required resources to effectively compute relevant inter-atomic interactions. Serious challenges exist with regard to qubit decoherence, noise, and the number of qubits. As such, the current state of quantum computers is commonly referred to as Noisy Intermediate Scale Quantum (NISQ). These challenges limit the capabilities in terms of capacity, as the number of qubits relates to the number of molecular orbitals that can be simulated. Currently, the largest systems boast in the order of ~ 1000 qubits. The maximum circuit depth is also a serious limitation, as recent publications have demonstrated the effort needed to simulate C_2H_4 (28 qubits).¹¹ To overcome these challenges in the near term, quantum algorithms need to make more efficient use of the available resources.

Most commonly, the approach to compute the ground state of a system is the variational quantum eigensolver (VQE).^{12,13} In variational algorithms, a parameterized quantum ansatz is evaluated for a cost function. The values of the parameters are updated through a classical optimizer until the cost function converges. This feedback loop requires computationally expensive classical-to-quantum feedback, which significantly impedes the efficiency of this algorithm. To this end, various approaches have been proposed to make the classical optimizer more efficient.¹⁴

To find more efficient algorithms, adaptations to VQE have been proposed using machine learning. Machine learning has been applied in various forms for largely omitting the parameter optimization through learning the parameters through classical neural networks.¹⁵⁻¹⁸ Machine learning has also been integrated with quantum computing to different ends. To combat the limitations of the number of qubits, quantum circuits have been developed to compress quantum information, specifically, the quantum auto-encoder (QAE).¹⁹⁻²² The QAE is a trainable parameterized quantum circuit (PQC), which reduces the number of

qubits required to store quantum information. This method is a quantum analog of the variational auto-encoder,²³ which compresses information into less data. In this work, instead of only compressing the molecular information, we will utilize the compression capabilities of the QAE to reduce the resource requirements of VQE circuits.

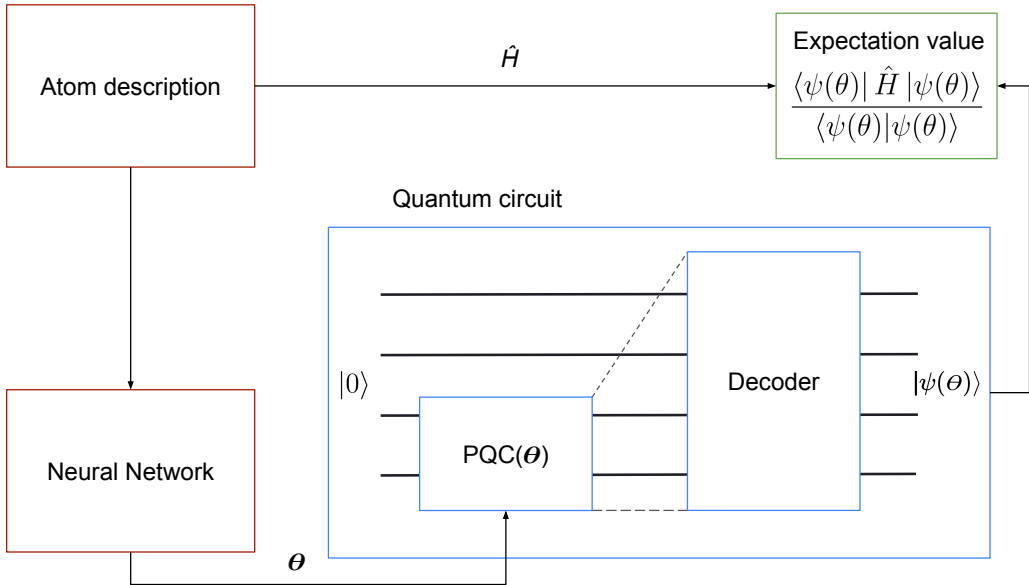


Figure 2: Overview of the VQE compression scheme.

In this work, we aim to optimize the VQE algorithm through a combination of QAE to reduce the number of qubits and apply a PQC on the latent quantum space. A classical neural network will be trained to predict the parameters of the PQC. For conciseness, we abbreviate this hybrid adaptation of VQE as NN-AE-VQE. The structure is schematically shown in Figure 2. This novel integration of VQE and quantum auto-encoding aims to achieve:

- Temporarily reduce the number of qubits for better algorithm scheduling;
- Reduce the number of circuit parameters to be trained;
- Reduce the overall circuit length to allow for larger electronic structures to be simu-

lated.

For the electronic structure calculations, the error rate needs to be below chemical accuracy (1 kcal/mole \approx 0.00159 Hartree).

With the proposed algorithm structure, we introduce a framework to systematically reduce the required resources for electronic structure calculations on a quantum computer. This alleviates the current limitations of NISQ quantum computers, aiming to utilize the efficiency of quantum computing in practical applications in the near term.

as a proof of concept, and compared to baseline VQE implementations. This method used is detailed in Section 2. The proposed model is tested on an H_2 problem as a proof of concept, and compared to baseline VQE implementations. These results are laid out in Section 3. From these results, advantages, limitations and future work will be discussed in Section 4. Finally the paper will be concluded in Section 5.

2 Method

In this paper, we use a variational algorithm to calculate the eigenvalues of a system Hamiltonian (VQE), adapted to be applied in a compressed quantum state. The motivation for compressing a variational algorithm is to temporarily reduce the required number of qubits, limit the algorithm depth, and reduce the number of parameters. This compression will be done through a Quantum Auto-Encoder (QAE).¹⁹ Furthermore, we train a classical neural network to predict the parameters of the compressed PQC. This way, we shift the computationally expensive parameter optimization to a re-usable offline trained model. Several intermediate steps are taken to integrate all elements. This includes training a quantum autoencoder, constructing a highly expressible but trainable parameterized quantum circuit (PQC), and setting up and training a classical neural network for the parameters. These steps will be explained in further detail to be combined in the final model.

2.1 Quantum Auto-Encoding

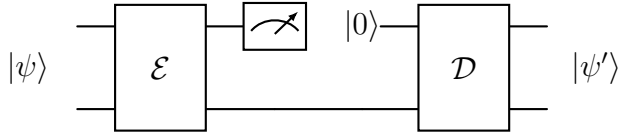


Figure 3: Basic structure of a QAE. A quantum state is encoded, after which the trash (upper) state is traced away, leaving only the encoded state (latent space). This encoded state is decoded back into its original state space using the decoder gate, of which the top (trash) input state is initialized with $|0\rangle$.¹⁹

The compression of the variable quantum circuit will be done through QAE. With QAE, similar to a classical auto-encoder, information is compressed to a dense form and can be decompressed to its original space. QAE aims to reduce the number of qubits to represent the information while minimizing the information loss. In this work, we will use the method presented by Romero et al.¹⁹ The overall structure is presented in Figure 3. With a QAE, a parameterized encoder and decoder are used to compress an initial quantum state to fewer qubits, which can be recovered to the original state using the decoder; the inverse of the encoder. The encoder is constructed from a parameterized quantum circuit, trained using a set of representable initial states. For these instances, a classical optimization is used to find the best parameter set for minimal information loss. In this paper, the initial state is the solved ground state of a Hydrogen molecule for a given atomic distance. The state is prepared through a UCCSD VQE ansatz with pre-trained parameters. After the encoding state, the "trash" state, i.e., the qubits discarded after encoding, should always produce a $|0\rangle$ state. This $|0\rangle$ state is re-instantiated for the decoding state to decode the compressed state back to the initial state. As can be seen in Figure 3, if the trash state equates to exactly $|0\rangle$, and the decoder is equal to the inverse of the encoder, both stages should cancel each other resulting in matching initial and final quantum state (i.e., $F(|\psi_i\rangle, \rho_i^{out}) = 1$). To train the decoder, it suffices to train the encoder and decoder using only the trash state.¹⁹ This method is also employed in this work, using a statevector simulator. To evaluate the trash state, the qubits in latent space are traced away, and the fidelity of the trash state is

extracted. On physical quantum hardware, a SWAP test²⁴ should be used to compare the 'trash' state to a reference state $|0\rangle$.

Moreover, several different quantum states must be used in training to ensure good accuracy over a range of quantum states. In this work, we use six random states to train the circuit. The quantum circuits are evaluated using a state-vector simulation, as a proof of concept.

2.2 PQC in latent space

In this work, we explore the usage of applying an ansatz in the latent space. With a pre-trained QAE, a parameterized quantum circuit (PQC) can be applied to the encoded quantum state. Several approaches can be taken to construct the PQC, such as a hardware-efficient modular circuit,²⁵ or an application-specific adaptive PQC²⁶ and others.¹³ For our approach, a more generic PQC is required, as the structure of the encoded quantum data is not fully determined. In this work, a pre-defined structure, specifically the *strongly entangled* ansatz,²⁷ is used as an expressive, but heuristic (generic) PQC. This PQC is shown in Figure 4. While this PQC ensures enough expressivity, which is especially relevant for an encoded state space, it could be further optimized to reduce circuit depth.

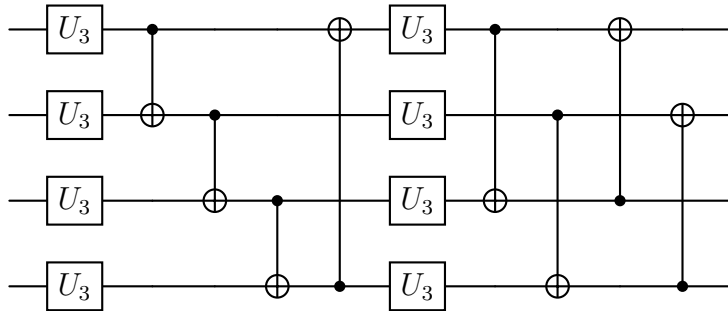


Figure 4: Circuit of the fully entangled PQC for 4 qubits.

In the used ansatz, the gate U_3 , a generic 3-angle (θ, π, γ) single qubit gate, is expressed as:²⁸

$$U_3 = \begin{bmatrix} \cos(\frac{\theta}{2}) & -e^{i\lambda} \sin(\frac{\theta}{2}) \\ e^{i\phi} \sin(\frac{\theta}{2}) & e^{i(\phi+\lambda)} \cos(\frac{\theta}{2}) \end{bmatrix} \quad (1)$$

For n qubits, the ansatz uses $2n$ single qubit gates (U_3) and $2n$ 2-qubit gates (CNOT), with $6n$ parameters.

2.3 Training the AE-VQE

Using a classical neural network to predict VQE parameters has been demonstrated before, e.g., by Tao et al.¹⁷ Here, a UUCSD ansatz is used for VQE,^{12,29} and a simple neural network is trained to predict the parameters. In this work however, the training will be significantly more challenging as the ansatz is more expressive.³⁰

The training of the PQC in combination with the QAE is shown schematically in Figure 5. First, the PQC is applied to a reduced $|0\rangle$ state, followed by the pre-trained decoder (inverse encoder). The circuit evaluation is done through state estimation for the H_2 Hamiltonian. Obtaining the training data will be expanded upon in Section 2.4.

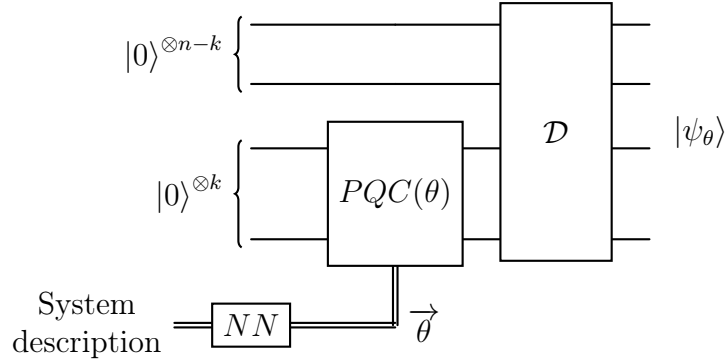


Figure 5: Using a classical neural network to predict compressed ansatz parameters. A classical optimizer first finds optimal values for the ansatz with a pre-trained decoder circuit. The found parameters are used to train a classical neural network.

Generating the training data for the neural network can be done through several configurations. These configurations are depicted in Figure 6. Three methods were considered for finding the optimal parameters for the trainable PQC. The initial approach was to directly

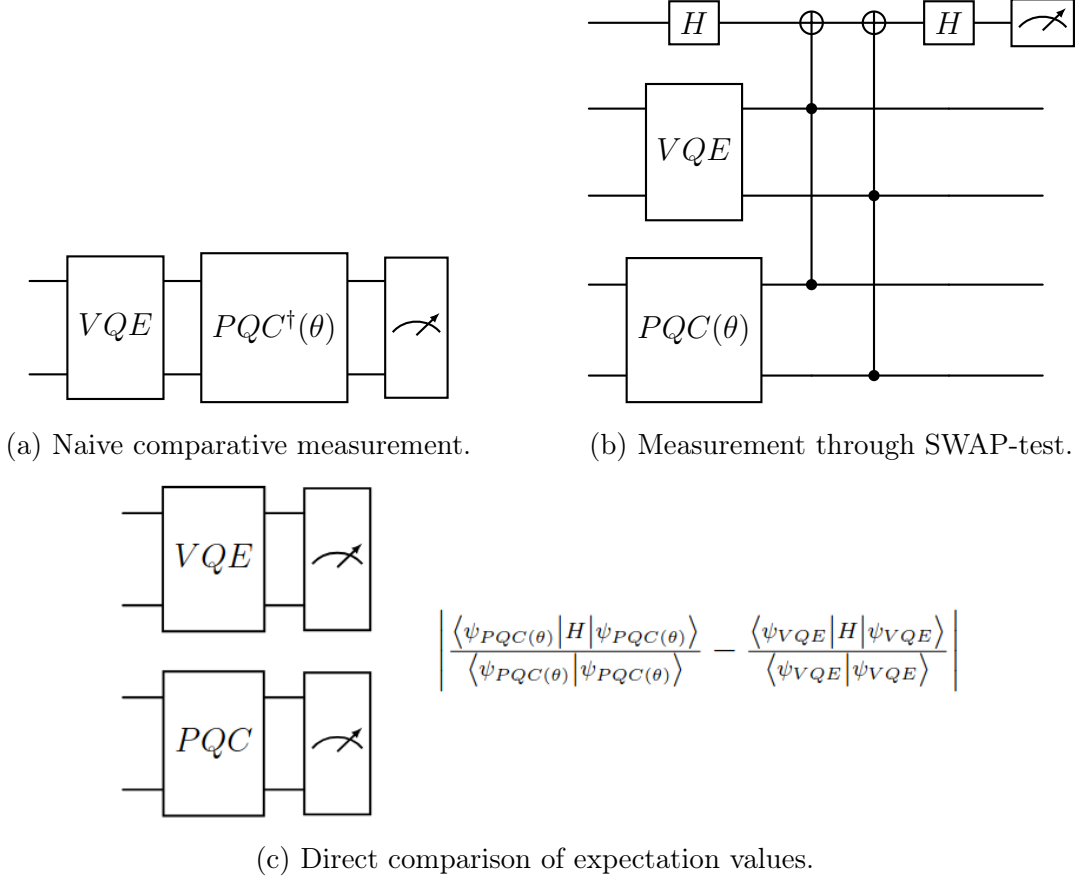


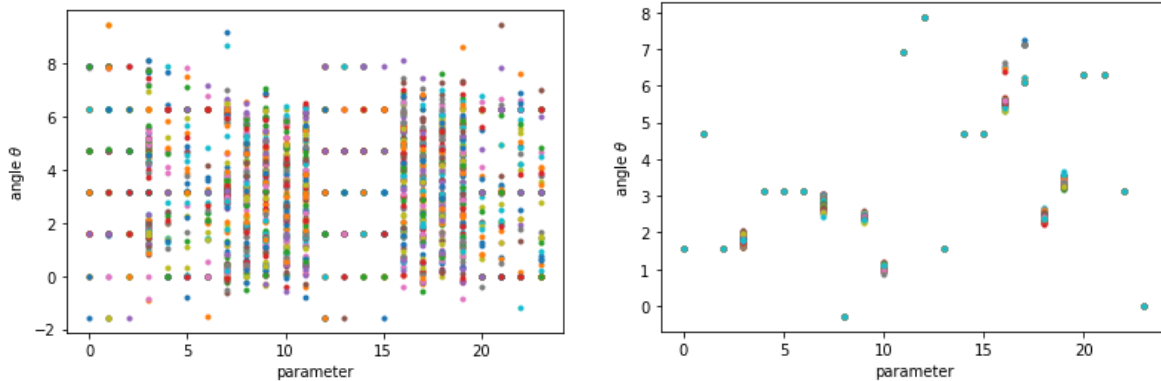
Figure 6: Alternative configurations for matching a PQC to a VQE state.

compare the pre-trained VQE ansatz with the inverse of the trainable PQC as shown in Figure 6a. If the VQE ansatz and $U^\dagger(\theta)$ are equal, one could naively expect to measure only 0, as both gates would cancel. However, training on this configuration makes for a deep quantum circuit. The second approach is through a SWAP-test, as depicted in Figure 6b. This method significantly reduces the circuit depth, and only needs a single qubit measurement in the computational basis. The drawback of this method is the $2N + 1$ qubit requirement for an N -qubit system state. As a quantum simulator is used, the doubling of qubits vastly increases the runtime. The final approach is the most simple and direct, which also proved to be the most effective. In this method, the expectation value of the trainable PQC is compared to the (pre-trained) expectation value of the VQE ansatz (Figure 6c). This means only N qubits are needed at the time, with the VQE results pre-trained and stored

in a database. It should be noted, that while VQE is here used as an example, alternative methods of obtaining reference values can be used such as experimental data of high-fidelity classical calculations which can be extracted from available databases.

2.4 Parameter trainability

In order to train the classical neural network to predict the parameters, several improvements were needed to make the parameters learnable. The challenge posed by using a highly expressive ansatz is that, while the parameter optimizations converge with good accuracy, the found parameters are uncorrelated due to the large search space (Figure 7a). Most notably, the three parameters of the individual U3 gates find several parameter combinations for the same gate, and as a circuit, different gate combinations find a similar final state (i.e. local optima). This makes a simple neural network to average between these parameter values resulting in inaccurate results.



(a) Parameter angles obtained using the initial approach with random initialization, all parameters optimized at once. The results are largely uncorrelated for different sample points.

(b) Parameter angles obtained using a global warm start with sequentially optimized gates. The obtained samples are often equal or in the same range.

Figure 7: Optimized parameters for strongly entangled ansatz for the H-H bond, sampled from different bond distances. This example implementation is applied without a decoder (on the 4-qubit state) resulting in 24 parameters. Each plot contains around 100 samples of optimized points. The x-axis shows the index of the parameters, with the corresponding optimal angles on the y-axis.

Instead, a structured approach is presented to force similar parameters. First, a global optimum is required as an accurate reference. This can be done by allowing the optimizer to do a full search over all parameters for a single inter-atomic distance, as would be done naively. Secondly, all other training points need to be correlated to this point. This is done using the reference global optima as an initial training point. Thirdly, the U3 gates are optimized in parts to limit the search space. First, the U3 gate is limited to a U1 gate, which is a single qubit rotation over the Z-axis:

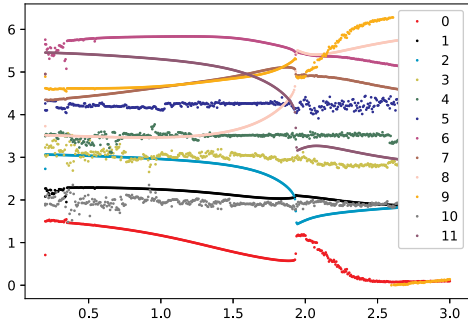
$$U1 = \begin{bmatrix} 1 & 0 \\ 0 & e^{i\lambda} \end{bmatrix} \quad (2)$$

This allows for optimizing only one parameter, assuring the optimization of different points will optimize in the same direction. After this partial optimization, the two locked parameters will be freed for optimization while the initial parameter is locked. Using this strategy, most parameters remain the same value for all points. The results are shown in Figure 7b, showing that even for different bond lengths, the angles remain close to each other for the same parameter.

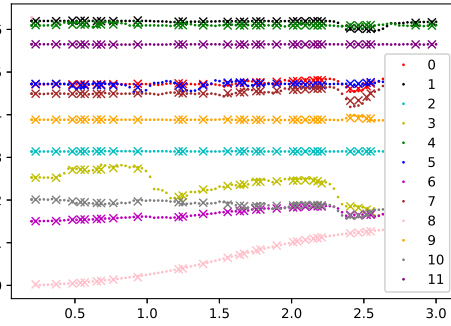
This, however, proved to be insufficient to produce accurate neural network predictions. The problem becomes clear when the parameters are plotted for the bond length, as shown in Figure 8a. In these results, it becomes clear that the parameter progression has a discontinuity, in this case around 1.95 Å. The actual value of this discontinuity has no relation to the physical system, as for different optimization passes, the position of the discontinuity changes. It is however consistent, that when parameters have discontinuities, the discontinuous point is the same for all parameters.

To avoid discontinuities, the parameter search is constrained in each step, such that for parameters $\vec{\theta}_t$ for time step t :

$$\vec{\theta}_t = \vec{\theta}_{t-1} + \delta \pm \alpha(\gamma + |\delta|), \quad \delta = \vec{\theta}_{t-1} - \vec{\theta}_{t-2} \quad (3)$$



(a) Parameter angles obtained using a global warm start with sequentially optimized gates.



(b) Parameter angles obtained using a global warm start with sequentially optimized gates. Additionally, the optimization steps are bound to ensure smoother parameter progression.

Figure 8: Optimized parameters for strongly entangled ansatz for the H-H bond, sampled from different bond distances. Each plot contains around 100 samples of optimized points. The x-axis shows the bond length, with the corresponding optimal angles on the y-axis. Parameters are presented by their index (0-11).

The result in Figure 8b no longer shows any discontinuity, allowing for better training. Still, the obtained parameters show that some parameters do not change, which could be used to simplify the ansatz. This would reduce the total number of parameters.

3 Results

In this section, we test against established algorithms and verify the accuracy, but also efficiency in terms of gates and parameters. To demonstrate the encoder and neural network model, we used an H_2 molecule as a minimal benchmark. Each element discussed in the previous section will be evaluated on accuracy. Furthermore, the impact on the efficiency will be discussed.

3.1 QAE results

The first step in establishing the model is training the QAE. As errors propagate in each step, it is crucial to ensure the QAE implementation achieves high accuracy. We demonstrate the compression of 4 qubits to 2, using the configuration shown in Figure 3.

With the training of the QAE a fidelity loss of the trash state of $4.46 \cdot 10^{-10}$ was achieved, which resulted in a mean absolute error (MAE) of the energy of $1.738 \cdot 10^{-7}$. This is within expectations, as the state fidelity is equal to or lower than the trash state fidelity, as stated by Romero et al. The currently found accuracy for the 4 to 2-qubit compression will be the maximum achievable accuracy for the training data.

3.2 NN-AE-VQA evaluation

We now evaluate the PQC ansatz in combination with the decoder to with the obtained training data. Using these parameters, we can evaluate the accuracy we can gain using a compressed ansatz. Furthermore, we use the results as training data for the classical neural network.

The neural network used for predicting the parameters is set up as a simple all-to-all sequential neural network, which uses the inter-atomic distance as the input value and VQA parameters as the output. The neural network is implemented with 4 hidden layers of each 30 nodes. Input values are normalized and output values are translated back to a 2π range. Additionally, to calculate the loss function the angles are translated to the squared distance of Cartesian coordinates, to ensure angle distances take rotational symmetry into account:

$$C = (\cos(\theta_{true}) - \cos(\theta_{pred}))^2 + (\sin(\theta_{true}) - \sin(\theta_{pred}))^2 \quad (4)$$

for parameter prediction θ_{pred} and actual value θ_{true} . Alternatively, the cosine similarity loss function can be used but performed slightly worse in our findings.

The training data for the neural network was generated by optimizing the parameters,

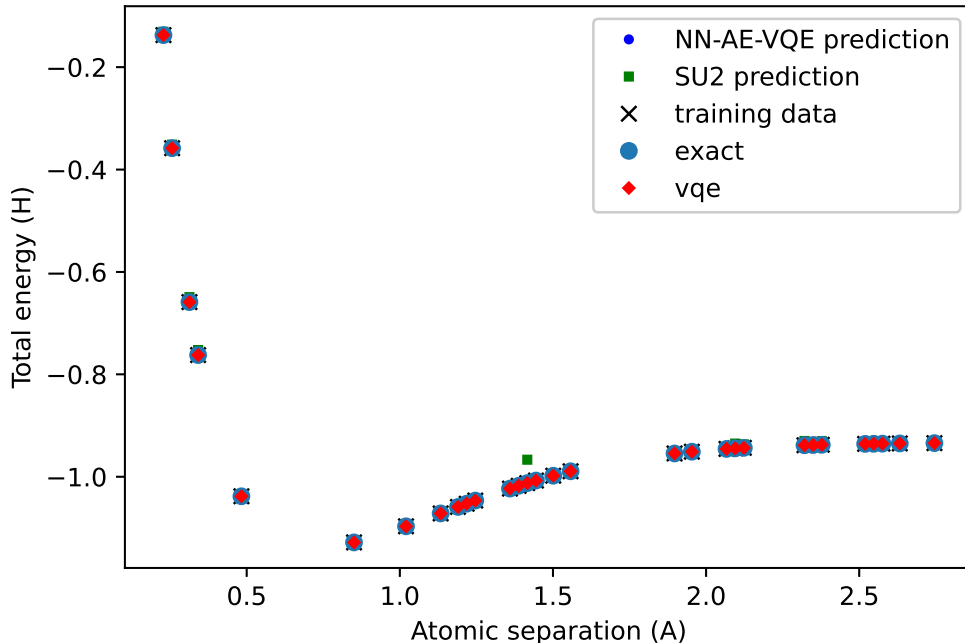


Figure 9: Comparison energy values for the H_2 molecule.

Table 1: Accuracy, gate requirements and number of parameters for different VQE implementations compared to (NN)-AE-VQE.

	MAE error	#gates	Parameters
efficient SU2	$7.170 \cdot 10^{-3}$	60	32
UCCSD	$1.563 \cdot 10^{-7}$	150	3
AE-VQE	$4.660 \cdot 10^{-7}$	6 + 36	12
NN-AE-VQE	$6.511 \cdot 10^{-5}$	6 + 36	12

starting from an optimal starting point. The remaining points are optimized using the warm start of the optimal point, using the constraints defined by Equation 3.

The results of the neural network predictions are benchmarked against the training data, the UCCSD ansatz and the SU2 ansatz.^{31,32} The UCCSD ansatz is known to be an accurate ansatz for VQE, but its circuit depth suffers from exponential scaling with the number of qubits. The efficient SU2 on the other hand is more of a heuristic ansatz, but is far more efficient in terms of scaling. Both the UCCSD and SU2 implementation are implemented directly from the Qiskit library.³³ The SU2 uses the default settings with a RY and RZ gate, and 3 repetitions. All results are compared to exact diagonalization.

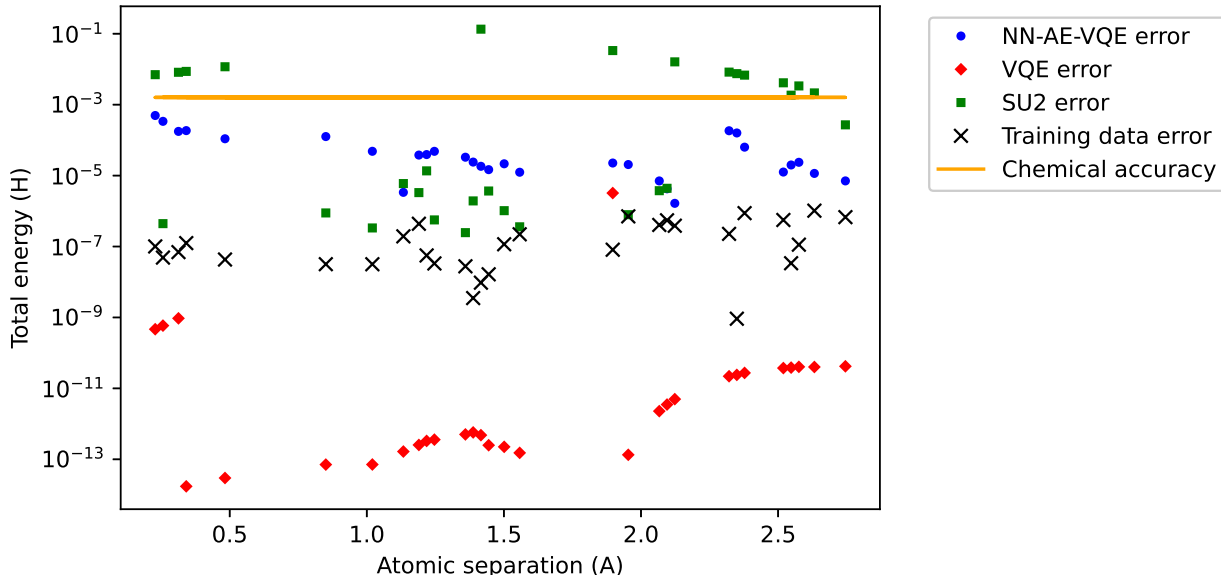


Figure 10: Comparison of error rates for 30 samples. The displayed methods are UCCSD VQE, SU2 VQE, the training data for the neural network, and the neural network predictions. The neural network training data is obtained for the PQC and the pre-trained QAE, optimized for the optimal values as described in section 2.4.

The results in Figure 10 and Table 1 show performance in line with expectations. The training data is noticeably less accurate compared to the VQE UCCSD reference results. Some of the error is induced by the decoder, having an accuracy of $1.738 \cdot 10^{-7}$. Logically, the neural network predictions give rise to more errors, with the limited accuracy of the parameter predictions. Despite these errors, the neural network results are well below the target chemical accuracy. Moreover, on average the neural network performs better compared to the SU2 results.

4 Discussion and outlook

In this chapter, we will discuss the additional measures that can be taken to improve upon the proposed method. One such improvement is the molecular encoding passed to the neural network. For simplicity’s sake, the current encoding is only the atomic distance. However, far more sophisticated methods are generally used for classical MLP, ensuring e.g. rotational

symmetry.⁷ This addition will be required for integrating this model in MD.

Currently, the number of gates scales quadratic with the number of qubits. This results in an unbalanced proportion of gates between the decoder and the PQC ansatz. To reduce this, ideally, a structure with linear entanglement should be used. The challenge is finding a QAE structure that still holds good accuracy. The *Real Amplitude* and *Efficient SU2* ansatz are examples of a more favorable scaling with a linearly growing number of 2-qubit gates. Other QAE implementations have also been presented in recent literature,^{21,22} which can be considered when aiming to improve the presented implementation. Another structure to consider is the quantum compression,^{20,34} where a lower order qubit compression ansatz is re-used, reducing the need to re-train parameters. Furthermore, the compression rate of the QAE is bounded by the problem Hamiltonian.³⁵ This needs to be taken into account when evaluating how much of an advantage can be achieved.

Regardless, a lower number of parameters are required when compressing the PQC. When the neural network predicted parameters are not sufficiently accurate, the prediction can still be used as a hot start for conventional optimization. This significantly reduces optimization time. The reduction of parameters through compression reduces the complexity, further accelerating the optimization.

The second possibility for improving the circuit ansatz is to do an ansatz circuit search.³⁶⁻³⁸ This method allows for the circuit to be optimized in terms of gates. Currently, several circuit optimization results have been found to have redundancy in terms of gates and parameters. Finding gates that stay constant for the same atomic configuration will allow for replacing parameterized gates with constant gates, which further saves neural network training for the parameters. Furthermore, for larger systems, the size of the circuit ansatz will be more significant, giving rise to the need to optimize in terms of circuit length.

A significant concern in this work is the structuring of parameters for training. Finding parameters in an increasingly more complex search space is considered one of the current prevalent challenges in variational quantum algorithms³⁹ (barren plateau). With the pre-

sented methodology, it could be explored how many similarities between different quantum problems are required to use a proxy or warm start for close convergence to the next problem. This is interesting in the use case discussed in this paper of relatively similar atom configurations, but could possibly be extended to graph problems where the structure is relatively consistent.

A further point to touch upon is investigating how similar the circuit ansatz parameters remain when changing the atom configuration. In our relatively simple case of the H_2 system, no drastic changes occur in changing the atomic distance. However, if we take the example of a phase change or excitation, the optimal circuit configuration could change as well. Further investigation is required as to how such mechanics will translate to the model predictions.

Another important element we would like to consider is the effect of increasing the (compressed) ansatz layers. In the current implementation, using a single layer proved to be effective for the test case. However, as is shown by Bravo-Prieto et al., the number of layers can find a critical point which significantly reduces the error rate.⁴⁰ Increasing the number of layers in the compressed space is favorable in terms of circuit depth compared to an uncompressed ansatz, therefore this could be an advantage to exploit.

Finally, we consider how to exploit the current quantum algorithm structure. One of the initial goals of this research was to reduce the number of qubits. In this work, we need to have a decoder of qubits equal to the number of qubit required in the original algorithm. This is required to sample expectation values in order to find a minimal eigenvalue. While there is no overall reduction for the algorithm as a whole, we can exploit the temporary decrease in qubits while in the compressed state. In the context of using the calculation in an ab-initio molecular dynamics setting, we expect to do many energy calculations in rapid succession. We can pipeline these instructions to achieve better efficiency, which was not possible in the original algorithm. A visual illustration of such a pipelining effort is shown in Figure 11. Here, the resource-intensive decoding stage can be executed in parallel with the resource-efficient variational algorithm. This means we can run 2 algorithm executions (mostly) in

parallel, using only $n + k$ qubits (n encoder qubits, k variational algorithm qubits). In the example of a 4-to-2 qubit encoding, only 6 qubits are needed instead of 8, with an extended runtime of one decoder depth.

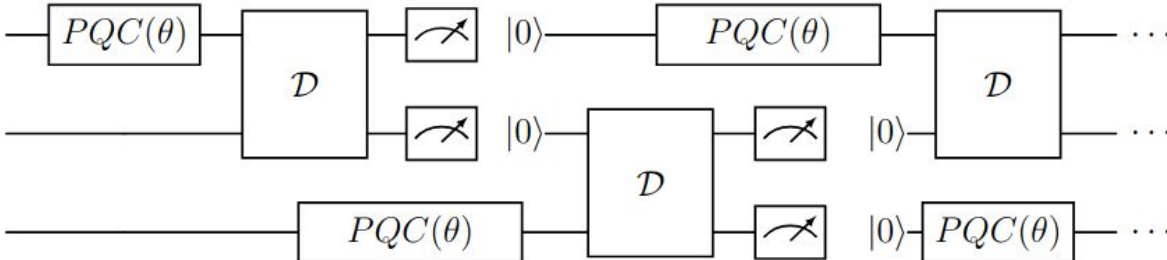


Figure 11: Possible pipelining structure for multiple VQE iterations using the compressed ansatz with decoder structure. For compactness, a 1-2 decompression is visualized but can be applied for other ratios such as 1-3, 2-4, etc.

Furthermore, the structure from Figure 11 becomes especially interesting when the depth of the PQC is close to the depth of the decoder (with measurement and qubit reset). For this, both efforts of creating a more efficient scaling of the decoder and exploring the increasing the PQC ansatz repetitions become especially relevant.

5 Conclusion

This work presents a novel approach to using a quantum auto-encoder to reduce the resources required for the VQE ansatz. Additionally, we provide a structured approach to preparing training data of the ansatz parameters for effective learning by a classical neural network. We demonstrate the accuracy of the proof-of-concept model, by testing the model on the H_2 molecule as a minimal working example. In the obtained results, we demonstrate an error rate well below chemical accuracy. With the proposed structure, we introduce a novel approach to constructing quantum variational circuits and introduce the exploitation of their unique advantages. Our methodology integrates VQE calculations more efficiently with molecular dynamics (MD) simulations, paving the way for significant improvements

compared to existing VQE implementations. By implementing QML in VQE, we demonstrate a more efficient trade-off of quantum resource requirements and accuracy. Reducing quantum resources will allow for larger molecular systems to be simulated while retaining chemical accuracy. Simulating both large samples and high accuracy is critical, especially for the high-impact areas of battery materials and HEA. Through these advances, we present progression toward a quantum advantage for high-accuracy MD simulations despite current hardware constraints.

References

- (1) Zhang, R.-Z.; Reece, M. J. Review of high entropy ceramics: design, synthesis, structure and properties. *Journal of Materials Chemistry A* **2019**, *7*, 22148–22162.
- (2) Oses, C.; Toher, C.; Curtarolo, S. High-entropy ceramics. *Nature Reviews Materials* **2020**, *5*, 295–309.
- (3) Zuo, Y.; Chen, C.; Li, X.; Deng, Z.; Chen, Y.; Behler, J.; Csányi, G.; Shapeev, A. V.; Thompson, A. P.; Wood, M. A.; others Performance and cost assessment of machine learning interatomic potentials. *The Journal of Physical Chemistry A* **2020**, *124*, 731–745.
- (4) Gilbert, M. R.; Arakawa, K.; Bergstrom, Z.; Caturla, M. J.; Dudarev, S. L.; Gao, F.; Goryaeva, A.; Hu, S.; Hu, X.; Kurtz, R. J.; others Perspectives on multiscale modelling and experiments to accelerate materials development for fusion. *Journal of Nuclear Materials* **2021**, *554*, 153113.
- (5) Bartlett, R. J.; Musiał, M. Coupled-cluster theory in quantum chemistry. *Reviews of Modern Physics* **2007**, *79*, 291.
- (6) Anstine, D. M.; Isayev, O. Machine Learning Interatomic Potentials and Long-Range Physics. *The Journal of Physical Chemistry A* **2023**, *127*, 2417–2431, PMID: 36802360.

- (7) Pinheiro, M.; Ge, F.; Ferré, N.; Dral, P. O.; Barbatti, M. Choosing the right molecular machine learning potential. *Chemical Science* **2021**, *12*, 14396–14413.
- (8) Mishin, Y. Machine-learning interatomic potentials for materials science. *Acta Materialia* **2021**, *214*, 116980.
- (9) Poulin, D.; Wocjan, P. Preparing Ground States of Quantum Many-Body Systems on a Quantum Computer. *Physical Review Letters* **2009**, *102*.
- (10) Lee, S.; Lee, J.; Zhai, H.; Tong, Y.; Dalzell, A. M.; Kumar, A.; Helms, P.; Gray, J.; Cui, Z.-H.; Liu, W.; others Evaluating the evidence for exponential quantum advantage in ground-state quantum chemistry. *Nature communications* **2023**, *14*, 1952.
- (11) Cao, C.; Hu, J.; Zhang, W.; Xu, X.; Chen, D.; Yu, F.; Li, J.; Hu, H.-S.; Lv, D.; Yung, M.-H. Progress toward larger molecular simulation on a quantum computer: Simulating a system with up to 28 qubits accelerated by point-group symmetry. *Physical Review A* **2022**, *105*.
- (12) Peruzzo, A.; McClean, J.; Shadbolt, P.; Yung, M. H.; Zhou, X. Q.; Love, P. J.; Aspuru-Guzik, A.; O’Brien, J. L. A variational eigenvalue solver on a photonic quantum processor. *Nature Communications* **2014**, *5*.
- (13) Hu, J.; Li, J.; Lin, Y.; Long, H.; Xu, X.-S.; Su, Z.; Zhang, W.; Zhu, Y.; Yung, M.-H. Benchmarking variational quantum eigensolvers for quantum chemistry. *arXiv preprint arXiv:2211.12775* **2022**,
- (14) Sweke, R.; Wilde, F.; Meyer, J.; Schuld, M.; Fährmann, P. K.; Meynard-Piganeau, B.; Eisert, J. Stochastic gradient descent for hybrid quantum-classical optimization. *Quantum* **2020**, *4*, 314.
- (15) Huang, R.; Tan, X.; Xu, Q. Learning to Learn Variational Quantum Algorithm. *IEEE Transactions on Neural Networks and Learning Systems* **2023**, *34*, 8430–8440.

- (16) Verdon, G.; McCourt, T.; Luzhnica, E.; Singh, V.; Leichenauer, S.; Hidary, J. Quantum Graph Neural Networks. 2019.
- (17) Tao, Y.; Zeng, X.; Fan, Y.; Liu, J.; Li, Z.; Yang, J. Exploring Accurate Potential Energy Surfaces via Integrating Variational Quantum Eigensolver with Machine Learning. *The Journal of Physical Chemistry Letters* **2022**, *13*, 6420–6426, PMID: 35816117.
- (18) Miao, J.; Hsieh, C.-Y.; Zhang, S.-X. Neural-network-encoded variational quantum algorithms. *Physical Review Applied* **2024**, *21*, 014053.
- (19) Romero, J.; Olson, J. P.; Aspuru-Guzik, A. Quantum autoencoders for efficient compression of quantum data. *Quantum Science and Technology* **2017**, *2*, 045001.
- (20) Anand, A.; Kottmann, J. S.; Aspuru-Guzik, A. Quantum compression with classically simulatable circuits. 2022; <https://arxiv.org/abs/2207.02961>.
- (21) Lamata, L.; Alvarez-Rodriguez, U.; Martin-Guerrero, J. D.; Sanz, M.; Solano, E. Quantum autoencoders via quantum adders with genetic algorithms. *Quantum Science and Technology* **2018**, *4*, 014007.
- (22) Bravo-Prieto, C. Quantum autoencoders with enhanced data encoding. *Machine Learning: Science and Technology* **2021**, *2*, 035028.
- (23) Rumelhart, D. E.; Hinton, G. E.; Williams, R. J. Learning representations by back-propagating errors. *nature* **1986**, *323*, 533–536.
- (24) Barenco, A.; Berthiaume, A.; Deutsch, D.; Ekert, A.; Jozsa, R.; Macchiavello, C. Stabilization of quantum computations by symmetrization. *SIAM Journal on Computing* **1997**, *26*, 1541–1557.
- (25) Kandala, A.; Mezzacapo, A.; Temme, K.; Takita, M.; Brink, M.; Chow, J. M.; Gambetta, J. M. Hardware-efficient variational quantum eigensolver for small molecules and quantum magnets. *Nature* **2017**, *549*, 242–246.

- (26) Ferrari, G.; Magnifico, G.; Montangero, S. Adaptive-weighted tree tensor networks for disordered quantum many-body systems. *Physical Review B* **2022**, *105*, 214201.
- (27) Schuld, M.; Bocharov, A.; Svore, K. M.; Wiebe, N. Circuit-centric quantum classifiers. *Physical Review A* **2020**, *101*.
- (28) Cross, A. W.; Bishop, L. S.; Smolin, J. A.; Gambetta, J. M. Open Quantum Assembly Language. 2017; <https://arxiv.org/abs/1707.03429>.
- (29) Romero, J.; Babbush, R.; McClean, J. R.; Hempel, C.; Love, P. J.; Aspuru-Guzik, A. Strategies for quantum computing molecular energies using the unitary coupled cluster ansatz. *Quantum Science and Technology* **2018**, *4*, 014008.
- (30) Holmes, Z.; Sharma, K.; Cerezo, M.; Coles, P. J. Connecting ansatz expressibility to gradient magnitudes and barren plateaus. *PRX Quantum* **2022**, *3*, 010313.
- (31) IBM Qisit circuit library EfficientSU2. <https://docs.quantum.ibm.com/api/qiskit/qiskit.circuit.library> 2024; [Online; accessed 04-11-2024].
- (32) Ganguly, S.; Yuvaraj, P. Efficient VQE Approach for Accurate Simulations on the Kagome Lattice. Artificial Intelligence and Knowledge Processing: Third International Conference, AIKP 2023, Hyderabad, India, October 6-8, 2023, Revised Selected Papers. 2024; p 397.
- (33) Javadi-Abhari, A.; Treinish, M.; Krsulich, K.; Wood, C. J.; Lishman, J.; Gacon, J.; Martiel, S.; Nation, P. D.; Bishop, L. S.; Cross, A. W.; Johnson, B. R.; Gambetta, J. M. Quantum computing with Qiskit. 2024.
- (34) Achache, T.; Horesh, L.; Smolin, J. Denoising quantum states with Quantum Autoencoders – Theory and Applications. 2020; <https://arxiv.org/abs/2012.14714>.

- (35) Ma, H.; Huang, C.-J.; Chen, C.; Dong, D.; Wang, Y.; Wu, R.-B.; Xiang, G.-Y. On compression rate of quantum autoencoders: Control design, numerical and experimental realization. *Automatica* **2023**, *147*, 110659.
- (36) Bilkis, M.; Cerezo, M.; Verdon, G.; Coles, P. J.; Cincio, L. A semi-agnostic ansatz with variable structure for variational quantum algorithms. *Quantum Machine Intelligence* **2023**, *5*, 43.
- (37) Du, Y.; Huang, T.; You, S.; Hsieh, M.-H.; Tao, D. Quantum circuit architecture search for variational quantum algorithms. *npj Quantum Information* **2022**, *8*, 62.
- (38) Kuo, E.-J.; Fang, Y.-L. L.; Chen, S. Y.-C. Quantum architecture search via deep reinforcement learning. *arXiv preprint arXiv:2104.07715* **2021**,
- (39) McClean, J. R.; Boixo, S.; Smelyanskiy, V. N.; Babbush, R.; Neven, H. Barren plateaus in quantum neural network training landscapes. *Nature communications* **2018**, *9*, 4812.
- (40) Bravo-Prieto, C.; Lumbrecas-Zarapico, J.; Tagliacozzo, L.; Latorre, J. I. Scaling of variational quantum circuit depth for condensed matter systems. *Quantum* **2020**, *4*, 272.